Three-Dimensional Analytical Model of Servovalve Torque Motor Using Reluctance Network

Marion Ribout, Carole Hénaux, Jean-François Llibre, Frédéric Messine, Batoul Attar

Three-Dimensional Analytical Model of Servovalve Torque Motor Using Reluctance Network

Marion RIBOUT[1,3], Carole HENAUX[2], Jean-François LLIBRE[1], Frédéric MESSINE[1], Batoul ATTAR[3]
[1]LAPLACE, CNRS, INPT, UPS, Université de Toulouse, 31077 Toulouse, France
[2]IES, Université de Montpellier, 34090 Montpellier, France
[3]Fluid Actuation and Control Toulouse (FACT), 31240 L'Union, France

***Abstract*— Electrohydraulic servovalves used in various aircraft systems (flight control system, auxiliary power unit, etc.) are a key element in fluid flow and pressure control. This paper presents a 3-D analytical modelling method of the electromagnetic performance of servovalves torque motor. This analytical model, based on a reluctance network, allows to quickly evaluate the actuator performance taking into account the complex 3-D geometry and the high flux leakage rate. This model enables to reduce the performance analysis time by about 89% compared to the conventional 3-D finite element calculation time. This is valuable for the design and optimization of the actuator geometry.**

Keywords*— *Torque Motor, 3-D Analytical Equivalent Magnetic Circuit, Magnetic Flux Leakage

I. Introduction

The purpose of the study is to present a more accurate analytical model of an actuator called torque motor which is commonly used in electrohydraulic servovalves. The idea is to use, in a future work, this model for torque motor design optimization. The proposed analysis method for determining motor performance saves computation time compared to a finite element software. The difficulty in implementing such a model lies in the need to represent a 3-D actuator which has many flux leakages as shown in Fig. 1. A reluctance model which takes into account the 3-D geometry of the actuator is proposed.

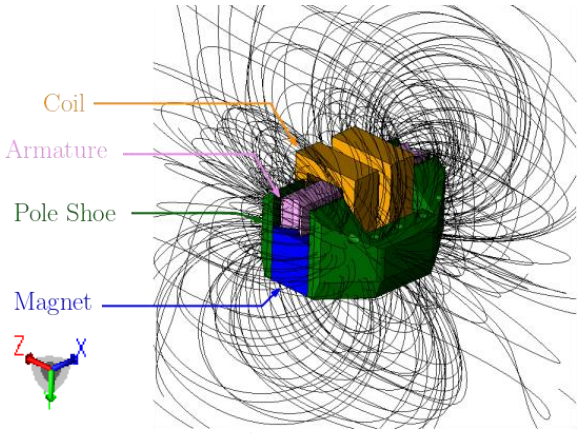

Fig. 1. Studied torque motor and flux leakage visualization [1]

Several studies have already been carried out. Merritt [2] has developed a simple analytical model of the actuator electromagnetic behavior which is still widely used. However, this model is not accurate as neither the magnet reluctance nor the leakage reluctances are taken into account. Urata [3], Liu [4] and Zhang [5] have improved it by integrating the magnetic characteristics of the magnet, flux leakages and the permeability of the yokes. However, these latter models cannot be used in an optimization process as an adjustment with experimental data is required each time the geometry is modified, hence the interest in developing a new analytical model without any need for recalibration. The study focuses on modeling the flux leakage without considering the magnetization curves of the soft ferromagnetic parts nor their saturation limits, i.e. considering their relative permeability infinite.

Fig. 2 shows a simple schematic 2-D view of the actuator under study. The actuator consists of two fixed iron parts, two magnets and a moving iron part supporting two coils fed along the same magnetization axis and separated by the pivot axis.

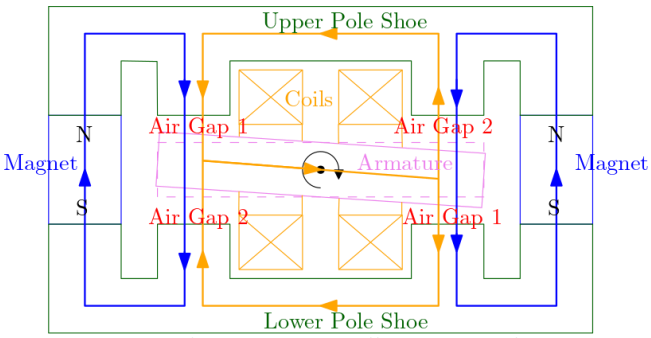

Fig. 2. 2-D diagram of the actuator with different magnetic fluxes

The developed torque in the actuator depends on the current intensity I consumed by the coils (N turns each), as well as the reluctance effect inherent to the movement of the armature relative to its centered position (θ). It is calculated either by determining the forces applied to the armature by Maxwell's stress tensor or by using the principle of virtual work, whose general expressions are given in [6]. These methods are both based on the knowledge of the magnetic fluxes that passing through the actuator. In previous studies, the expression of the force applied to the armature, according to the Maxwell stress tensor, assumes that the tangential component of the magnetic field in the air gap is zero and that only the fluxes flowing in the air gaps generate a force.

II. Methodology of Analytical Models Development

The equivalent reluctant network developed in this study is used to model the main flux path through the air gaps and magnets and the leakage flux paths between the various ferromagnetic parts (Fig. 3).

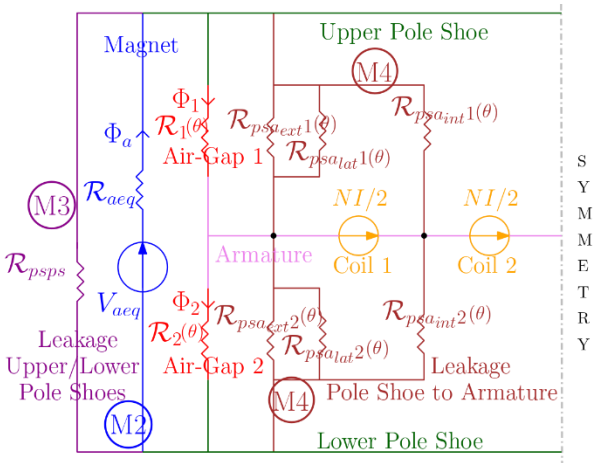

Fig. 3. Developed reluctance network model

The developed method provides a progressive improvement of the analytical model by iteratively integrating different types of leakage flux (Fig. 3). Four models are presented to highlight the impact of different leakages on the actuator electromagnetic torque estimation accuracy.

The magnetic potential and reluctance of the magnet are denoted V_a and $\mathcal{R}_a$ respectively, a coefficient k_a gives the relation $V_{aeq} = k_a V_a$ and $\mathcal{R}_{aeq} = k_a \mathcal{R}_a$. Φ_1, Φ_2, Φ_a are the magnetic fluxes passing through air gap 1, 2 and magnet respectively.

Model 1 (M1) is based on the Merritt model [2] that considers only the main flux path. Only the air gap reluctances $\mathcal{R}_{1,2}(\theta)$, as well as the coil and basic magnet model ($k_a = 1$) are taken into account. The M1 is still an improvement of what is done in [2] as the magnet reluctance has been added.

Model 2 (M2) implements a non-uniform magnetic induction in the magnet as introduced in [3], so an equivalent model of the magnet will be suggested ($k_a \in]0,1[$).

Model 3 (M3) adds the leakage fluxes that occur between the two pole shoes represented by the reluctance $\mathcal{R}_{psps}$ (shown in purple in Fig. 3).

Model 4 (M4) is enhanced by considering the leakage between the pole shoes and the armature. These leakages have the particularity of being introduced by variable reluctances that depend on the position of the armature. They can be divided into 3 types: $\mathcal{R}_{psa_{int}}(\theta)$, the leakage on the inner sides of the armature, $\mathcal{R}_{psa_{ext}}(\theta)$, the leakage on the outer end of the armature and $\mathcal{R}_{psa_{lat}}(\theta)$, the leakage on the top and bottom of the armature (shown in brown in Fig. 3).

A. *Modeling the flux leakage at magnet level (M2)*

The magnet is discretized into a number of layers n_a stacked along its magnetization axis. Each layer is assumed to be crossed by an uniform induction with a symmetrical evolution of the induction with respect to the central layer representing the middle of the magnet (Fig. 4). The leakage path can be assimilated to a half-circle, whose geometric parameters depend on the dimensions of the magnet.

Using the Thévenin and Norton theorems, an equivalent model of the magnet is determined, taking into account the modelled leakage path. The coefficient k_a is expressed as a mathematical series and converges to a finite value when n_a tends to infinity.

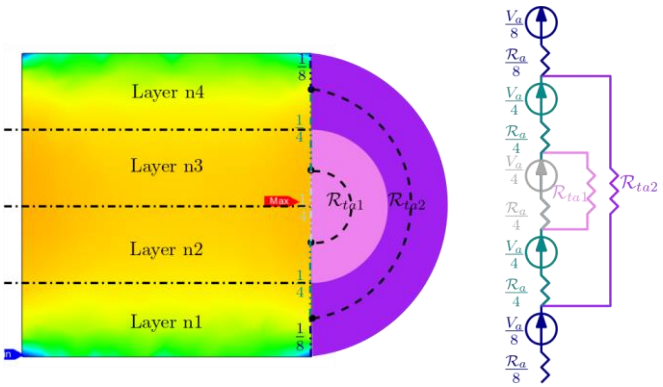

Fig. 4. Magnet modeling with several layers (example with 4 layers)

B. *Modeling of magnetic leakage between two iron parts (M3-M4)*

In M3-M4, the analytical expression of the leakage reluctance $\mathcal{R}_c$ that exist between two iron parts is required. It is therefore necessary to estimate the length l_c and cross-sectional area S_c of the flux tube as:

$$\mathcal{R}_c = \int_0^{l_c} \frac{dl}{\mu_0 S_c(l)} \quad (1)$$

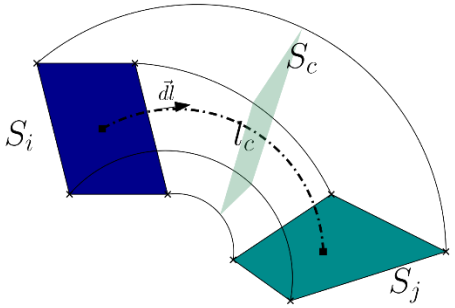

Fig. 5. Visualization of flux tube between two different surfaces

The modeling is based on a simplification of the possible shapes of a magnetic flux tube in air (Fig. 5). The shape of the tube is restricted to a 3-D ellipse denoted $\mathcal{E}$, which can be set mathematically according to the following equation: $\forall(x,y,z) \in \mathcal{E}$,

$$\frac{\left((x-u_x)\cos\varphi + (y-v_y)\sin\varphi\right)^2}{a^2} + \frac{(z-w_z)^2}{b^2} = 1 \quad (2)$$

with (u_x, v_y, w_z) the origin of the ellipse $\mathcal{E}$, φ the $\mathcal{E}$ rotation along the z-axis, a and b the semi-major and minor axis of ellipse $\mathcal{E}$. To obtain a non-tubular ellipse that can be represented in a 3-D plane, the following equation is used, $\forall(x,y,z) \in \mathcal{E}$:

$$\cos\varphi\,(y-v_y) = \sin\varphi\,(x-u_x) \quad (3)$$

It is assumed that these equations, whose unknowns are $(a, b, \varphi, u_x, v_y, w_z)$, can model all flux in accordance with the observed magnetic symmetries of the actuator. However, it is found that there are an infinite number of ellipses passing through random points in 3-D space.

To restrict the set of solutions of the problem, the discontinuity of the boundary condition of the tangential component of the magnetic field $\vec{H}$ between any two media A and B is added.

$$\left(\overrightarrow{H_A} - \overrightarrow{H_B}\right) \times \overrightarrow{n_{AB}} = \overrightarrow{J_s} \quad (4)$$

Considering that no free current density J_s exists at the iron-air interface and that the permeability of iron is high compared to that of air, we can assume that the magnetic field $\vec{H}$ is zero in iron (because the magnetic induction $\|\vec{B}\|$ is finite in iron). Thus, the tangential component of $\vec{H}$ is set to be zero at the air-side interface. This requires that the slope of the ellipse $\mathcal{E}$, which represents the magnetic leakage line, is normal to the leakage surface. This assumption is restricted by the fact that the iron should not be saturated at the interfaces.

The equations relating to the above assumptions are applied between two distinct surfaces of the actuator S_i and S_j, where the points considered $X_i : (x_i, y_i, z_i)$ and $X_j : (x_j, y_j, z_j)$ are the contour points of the two surfaces. Solving the problem enables to determine the length (ellipse arc perimeter) and cross-sectional area of the leakage flux tube

between two distinct surfaces and thus the values of the leakage reluctances (Fig. 5).

The cases of leakage between, first, the two pole shoes and, secondly, between the pole shoe and the armature are treated individually. Indeed, this two cases lead to two distinct situations in the resolution of the system of equations.

C. *Case of leakages between the two pole shoes (M3)*

The two pole shoes in the actuator are both symmetrical in the *(0xy)* plane. Only the points X_i and X_j which are symmetrical along this plane, admit a solution to the problem set. Nevertheless, solving the above system of equations leads to an infinite number of solutions (Fig. 6).

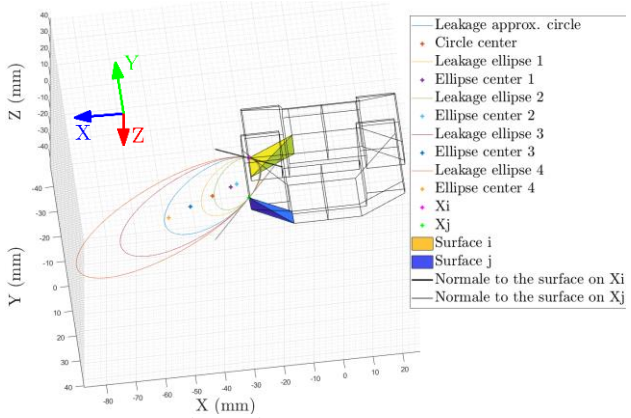

Fig. 6. Visualization of a set of possible ellipses that represent the leakage

The aim of our model is to obtain a unique and repeatable model of the flux tube. The methodology applied is to consider that there are two ellipses with a minimum and maximum perimeter for each pair of surfaces studied. This defines the minimum and maximum length of the flux tube between these two surfaces. An average length is then associated with the studied flux tube.

In order to find the minimum perimeter, the ellipse is not allowed to cross any iron part, which means that the leakage flux tube must remain in the air. The minimum coordinates of the ellipse is set to $(x_{min}, y_{min}, 0)$. To find the maximum perimeter, the flux line is bound to remain in an air box of finite size, larger than the dimension of the actuator (in this case 2.5 times larger). Thus, the maximum coordinates of the ellipse is set to $(x_{max}, y_{max}, 0)$. In Fig. 7, the blue zone represents the maximum cross section area for the leakage flux outside the actuator in *(0xy)* plane and the yellow zone is the maximum cross section area for the leakage flux inside the actuator in *(0xy)* plane. The leakage flux tube is included in these areas as it passes through the *(0xy)* plane.

The cross section of the flux tube is assumed to vary linearly between the leakage area in the iron and the area of the tube in the *(0xy)* plane. This latter area depends on the previously defined limits, and is located between the actuator and the specified air box. Note that it is important to avoid considering the same leakage area multiple times, as this would lead to an underestimation of the leakage reluctance. Indeed, for different pairs of surfaces, it is possible that the flux tubes passing in the *(0xy)* plane share the same passage zone. In this case, it is possible to simultaneously treat several pairs of surfaces whose leakage pass through the same zone in order to simplify the problem.

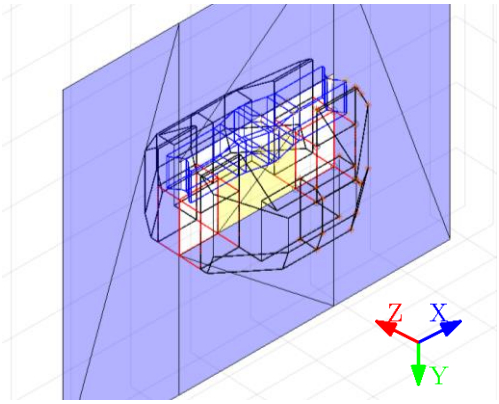

Fig. 7. Maximum cross-section area of the magnetic flux tube in *(0xy)* plane

D. *Case of leakages between pole shoe and armature (M4)*

In the case of leakage between pole shoe and armature, the *(0xy)* plane is no longer a symmetry plane for the surfaces under study (e.g. Fig. 8). The system of equations can only be solved by a unique solution, or no solution at all. The effective leakage surface is determined by the position of the contour points of the surface that allow a solution to the problem under study.

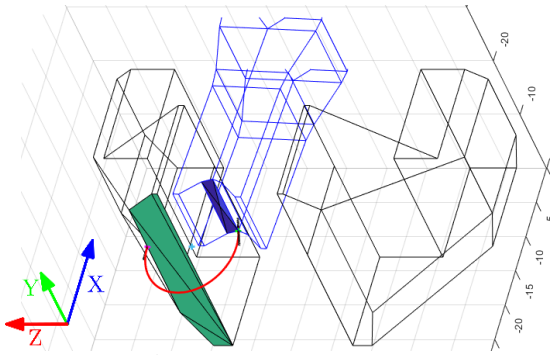

Fig. 8. Visualization of a leakage line between pole shoe and armature

For a given couple of surfaces, an average length of flux tube is determined and the cross-section of the tube is assumed to vary linearly between the effective surface area of the leakage from the pole shoe to that of the armature.

III. Validation of Analytical Model

The different analytical models are validated by comparing their results with the results obtained by JMAG® for a given geometry. It should be noted that the experimental results obtained on the test bench for the whole system agree well with the results of the finite element software.

For the actuator under study, the magnetic induction remains below saturation limit according to JMAG® simulation. Regarding the used ferromagnetic material, it can be deduced, from the maximum induction reached, that the relative permeability remains very high (>1e4). The impact of the iron reluctance is therefore low on the actuator magnetic performance and the assumption for modelling the leakage lines remains consistent. For an optimization process, however, magnetic induction modeling is mandatory to avoid magnetic saturation issues. In a such geometric construction, magnetic induction cannot be approximated to its normal component which is related to the magnetic flux. The estimation of tangential component is required to accurately model the magnetic induction in the actuator. This issue will be addressed in further work.

The improvement in actuator performance modeling accuracy is assessed for the four successive models. Model 4 provides the most accurate depiction of the magnetic fluxes passing through the magnets and air gaps as shown in Table I. However, it is noted that the deviation for air gaps magnetic fluxes (and in particular from air gap 2) remain significantly even at zero angle. This difference can be explained by the approximate calculation of the leakage reluctances in 3-D, but also by the position of the reluctances in the equivalent reluctance network.

TABLE I. MAGNETIC FLUX EVOLUTION BASED ON THE MODEL USED

	$i = 0.3A / \theta = 0°$			$i = 0.3A / \theta = 3°$		
	Φ_1 (Wb)	Φ_2 (Wb)	Φ_a (Wb)	Φ_1 (Wb)	Φ_2 (Wb)	Φ_a (Wb)
Model 1	$1.23e^{-4}$	$9.82e^{-5}$	$1.11e^{-4}$	$1.67e^{-4}$	$6.83e^{-5}$	$1.18e^{-4}$
Model 2	$1.05e^{-4}$	$8.02e^{-5}$	$9.27e^{-5}$	$1.44e^{-4}$	$5.63e^{-5}$	$1.00e^{-4}$
Model 3	$5.67e^{-5}$	$3.18e^{-5}$	$1.54e^{-4}$	$7.96e^{-5}$	$2.27e^{-5}$	$1.56e^{-4}$
Model 4	$5.37e^{-5}$	$2.88e^{-5}$	$1.57e^{-4}$	$7.55e^{-5}$	$2.06e^{-5}$	$1.59e^{-4}$
JMAG®	$4.92e^{-5}$	$2.18e^{-5}$	$1.57e^{-4}$	$6.64e^{-5}$	$1.65e^{-5}$	$1.58e^{-4}$

Two methods of computing the electromagnetic torque are used: the Maxwell stress tensor (**A**) in agreement with the expression used in [2]–[5] and the virtual work method (**B**). The results given in TABLE II. show the torque modelling deviation comparing to JMAG® using both methods and following the expression:

$$err = \left(\Gamma^{\text{Model}}(I,\theta) - \Gamma^{\text{JMAG}}(I,\theta)\right)/\Gamma^{\text{JMAG}}(I_{nom}, 3°) \quad (5)$$

Here, coils are supplied with the rated current (0.3A).

TABLE II. TORQUE MODELING DEVIATION COMPARED TO JMAG®

err (%)		$\theta = -3°$	$\theta = 0°$	$\theta = 3°$
Model 1	**A**	-252.7	66.7	402.9
	B	-214.1	65.6	348.4
Model 2	**A**	-166.6	48.4	280.0
	B	-138.1	47.4	237.5
Model 3	**A**	-23.0	-1.1	25.6
	B	-16.6	-1.6	11.4
Model 4	**A**	-18.7	-4.1	13.8
	B	-13.9	-4.5	2.1

As TABLE II. depicted, the accuracy of the estimated torque has been improved progressively with model enhancement. However, the use of Maxwell stress tensor, using the assumptions of previous studies described in I, can be questioned by the presence of leakage between the pole shoes and the armature, which contributes to the generation of torque, as well as the presence of the magnetic field tangential component in the air gap for non-zero armature pivot angles (the flux lines being modelled by ellipses).

Using magnetic coenergy to calculate the torque shows an improvement in the accuracy of the modelling, especially at high angles with the increase of leakage dissymmetry and the occurrence of a tangential component in the air gaps.

TABLE III. describes the evolution of the accuracy achieved by successive improvements of the model using magnetic coenergy to estimate the torque. The armature movement is between -3° and +3°. The characterization time (CPU time) corresponds to the time required to calculate the torque at a given current, from -3° to +3° by increments of 1°, whose evolution can be evaluated according to the model used.

TABLE III. ACCURACY AND CPU TIME OF THE DIFFERENT METHODS

	max(err) at $I = I_{nom}$ (%)	max(err) at $I = 0A$ (%)	Characterization Time– 7 points (s)
Model 1	348%	284%	0.8
Model 2	238%	190%	0.8
Model 3	17%	16%	1.1
Model 4	14%	10%	28-35

The needed time to characterize the actuator (e.g. for 7 points) using JMAG® software is 315s. This finite element analysis is done with the largest possible mesh size in order to limit the calculation time without any loss of accuracy. As TABLE III. depicted, the developed model M4 allows to converge to the JMAG® results with a much lower simulation time (up to 11 times faster for characterization time).

IV. CONCLUSION

In this paper, an enhanced analytical model is presented to predict the torque motor electromagnetic performance, whatever its geometry and without any need of reluctance recalibration with Finite Element Method (FEM) software, which is the major improvement regarding the literature. The purpose of this model is to be used in the torque motor design optimization process, which allows to reduce the characterization time. An incremental improvement of the analytical model is presented to show the enhancement of estimated torque. The results of these different analytical models are established by comparing them to a 3-D FEM software. This methodology enables fast pre-optimization of the structure to meet defined performance requirements. However, in an optimization process, it is worth to model the magnetization state of soft ferromagnetic parts to avoid their saturation at nominal operation. This issue is the topic of ongoing work.

The applied methodology can be used whenever elliptical flux tubes in air need to be accurately modeled to assess magnetic performance, regardless of actuator design as long as the iron is not saturated.

REFERENCES

[1] G. Ozzello, 'Servovalve for Regulating the Flow or Pressure of a Fluid', US-20210079934-A1, Mar. 18, 2021. [Online]. Available: https://image-ppubs.uspto.gov/dirsearch-public/print/downloadPdf/20210079934

[2] H. E. Merritt, *Hydraulic Control Systems*, John Wiley&Sons. 1967.

[3] E. Urata, 'On the torque generated in a servo valve torque motor using permanent magnets', *Proceedings of the Institution of Mechanical Engineers, Part C: Journal of Mechanical Engineering Science*, vol. 221, no. 5, pp. 519–525, May 2007.

[4] C. Liu and H. Jiang, 'Influence of magnetic reluctances of magnetic elements on servo valve torque motors', *Chin. J. Mech. Eng.*, vol. 29, no. 1, pp. 136–144, Jan. 2016.

[5] Q. Zhang, L. Yan, Z. Duan, Z. Jiao, C. Gerada, and I.-M. Chen, 'High Torque Density Torque Motor With Hybrid Magnetization Pole Arrays for Jet Pipe Servo Valve', *IEEE Trans. Ind. Electron.*, vol. 67, no. 3, pp. 2133–2142, Mar. 2020.

[6] J. Pyrhonen, T. Jokinen, and V. Hrabovcová, *Design of rotating electrical machines*. Chichester, West Sussex, United Kingdom ; Hoboken, NJ: Wiley, 2008.